Mathematical Biosciences and Engineering

MBE, 17(1): 216–234.
DOI: 10.3934/mbe.2020012
Received: 03 March 2019
Accepted: 18 August 2019
Published: 30 September 2019

http://www.aimspress.com/journal/MBE

Research article

Examining and monitoring paretic muscle changes during stroke rehabilitation using surface electromyography: A pilot study

Ge Zhu [1], Xu Zhang [1,*], Xiao Tang [1], Xiang Chen [1] and Xiaoping Gao [2,*]

[1] Department of Electronic Science and Technology, University of Science and Technology of China, Hefei, Anhui230027, China
[2] Department of Rehabilitation Medicine, First Affiliated Hospital of Anhui Medical University, Hefei, Anhui230022, China

* **Correspondence:** Email: xuzhang90@ustc.edu.cn, gxp678@163.com.

Abstract: Complex neuromuscular changes have been reported to occur in paretic muscles following stroke, but whether and how they can recover under rehabilitation therapy remain unclear. A tracking analysis protocol needs to be designed involving multiple sessions of surface electromyography (sEMG) examinations during the rehabilitation procedure. Following such a protocol, this pilot study is aimed to monitor paretic muscle changes using three sEMG indicators namely clustering index (CI), root mean square (RMS) and medium frequency (MDF). Initially, a single sEMG examination was performed on the abductor pollicis brevis (APB) muscle on both sides of 23 subjects with stroke and one side of 18 healthy control subjects. With these data to establish CI diagnostic criterion, the paretic muscles of all subjects with stroke showed a very board CI distribution pattern from abnormally low values through normality to abnormally high values. Afterwards, 9 out of 23 subjects with stroke had their paretic muscles examined at least twice before and after the treatment. Almost all paretic muscles had an increase of the RMS, a change of the MDF approaching to the value of the contralateral muscle, and a change of the CI returning to its normal range after common rehabilitation treatments. Finally, 4 of the 9 subjects with stroke participated into repeated examinations of their paretic muscles. The combined use of three indicators helped to reveal specific neuromuscular processes contributing to recovery of paretic muscles, due to their complementary diagnostic powers. Furthermore, neuromuscular processes were found to vary across subjects in type, order and timing during rehabilitation. In conclusion, given the 4 cases following the tracking analysis protocol, this pilot study preliminarily demonstrates usability of three sEMG indicators as tools for examining and monitoring stroke rehabilitation procedure in terms of improvements of paretic muscle changes. All the revealed complex neuromuscular processes imply the necessity of

applying sEMG examinations in monitoring rehabilitation procedure, with the potential of offering important guidelines for designing better and individualized protocols toward improved stroke rehabilitation.

Keywords: paretic muscle monitoring; surface electromyography; neuromuscular changes; stroke rehabilitation; noninvasive examination

Abbreviations: sEMG: surface electromyography; CI: clustering index; RMS: root mean square; MDF: medium frequency; APB: abductor pollicis brevis; B stage: Brunnstrom stage; F-M: Fugl-Meyer; EMG: electromyography; MU: motor unit; MUAP: motor unit action potential; MAS: modified Ashworth scale; MVC: maximal voluntary contraction; *Rm*: mean residual; SD: standard deviation

1. Introduction

Stroke is the leading cause of acquired disability in adults in most countries [1]. Two-thirds of stroke survivors suffer from moderate or severe disability within five years, with various body-functioning impairments including muscle weakness, spasticity, and abnormal motor coordination, which have disproportionate impact on the living quality of patients with stroke [2,3]. Although neurological damage is often irreversible, motor function is proven to probably recover well with effective rehabilitation intervention as early as possible [4–6]. As stroke population has been growing, the urgent demand of rehabilitation health-care has driven substantial amount of researches into understanding mechanisms associated with complex neuromuscular processes of post-stroke rehabilitation [7–11].

A varieties of scales have been routinely used to evaluate motor function, mainly from its macroscopic appearance [12], including Brunnstrom stage (B stage) [13], Fugl-Meyer (F-M) Assessment [14], Barthel Index [15], and National Institutes of Health Stroke Scale [16–18]. Although tracking assessment could be easily performed by various clinical scales to monitor the improvement of motor function, it gives relatively subjective diagnosis as a result of lack in consensus between assessors [19]. More importantly, it only evaluates the degree of recovery for motor function [20] rather than provide sufficient information concerning recovery mechanism. Therefore, development of quantitative assessment methods, which can be used to evaluate motor performance as well as to explore the rehabilitation mechanisms of both central and peripheral nervous system, is driven by the aims at improved rehabilitation.

Noting that motor unit (MU) is the most basic functional unit and final pathway of neuromuscular control. Its structure, function and control property alternations are direct causes of motor impairment [21]. Thus it is of great importance to identify pathological changes in MU following stroke. Both bioptic studies [8,9] and clinical electromyographic studies (e.g., concentric needle electromyography (EMG) [22,23], electrical stimulation [24] and macro-EMG [25], etc) have been continuously conducted in this direction. These studies draw contradictory conclusions on involvement of spinal motoneurons and MUs after stroke, indicating their underlying complex mechanisms. Recently, more evidences have demonstrated that spinal motoneurons can be affected as a result of central motoneuron damage after stroke, leading to considerable denervation and

therefore re-innervation [8–11]. In these studies, however, invasive or painful procedures are involved. Thus, they are not suitable for multi-site measurement and long-term monitoring. Moreover, implementation of these techniques always requires participation of medical professionals, which restricts their wide applications in community or home.

Surface EMG (sEMG), as an alternative approach for electrophysiological examination, has attracted much research interest due to its noninvasive manner of measurement [26–28]. Although the sEMG always measures signals with lower signal-to-noise ratios than the invasive/needle EMG technique, it has all the basic research significance and clinical application potentials. Therefore, it is crucial to develop an algorithm to interpret the information convoyed in sEMG recordings effectively. Multiple methods for extracting information related to MU from sEMG has been proposed in broad research programs for clinical examination and diagnosis of neuromuscular diseases [27,28]. Simple amplitude-associated parameters such as root mean square (RMS) [29], mean rectified value [30], and peak amplitude distribution [31] can be used to illustrate the magnitude of muscle strength. Frequency-domain parameters such as median frequency (MDF) [32] and mean frequency [29,33] can be used for assessment of neuromuscular changes resulted from both peripheral and central factors. As reported in literature, the changes in spectral structure of sEMG may be associated with alternations of MUs in structure and type and their central control properties, i.e., the simultaneous firing of motor unit action potential (MUAP), the firing rate and the change of recruitment mode [34]. In addition, some researchers use time-frequency parameters (e.g., wavelet transform [35]) and nonlinear parameters (e.g., entropy [36–38]) to extract information related to MU alternations from sEMG.

In recent years, clustering index (CI) analysis has been further confirmed to have high sensitivity to quantitatively discriminate neurogenic and myopathic changes [39,40]. Compared with the other sEMG analyses reporting differences at the group level, CI has capability of producing diagnostic decisions at the individual muscle level. Our previous work [41] adopted the CI method to explore the complex neuromuscular changes post-stroke, presenting possible contributors of MU alternations to neurogenic changes and myopathic changes. However, most studies including our previous work mainly focused on neuromuscular change examination at a single time point rather than tracking or monitoring the improvement of neuromuscular status during rehabilitation. Specifically, rehabilitation is a long-term process during which its mechanisms underlying muscle function recovery still remain unknown. Therefore, it is necessary to conduct continuous monitoring of the rehabilitation procedure so as to offer better understandings regarding recovery of paretic muscles.

Beyond the previous findings mentioned above, we further hypothesize that there are complex and neuromuscular processes underlying the improvement of pathological changes as a result of stroke during the rehabilitation procedure, and that these processes can be effectively visualized by sEMG indicators such as CI, RMS and MDF. In order to verify this hypothesis, the paretic muscles were continuously monitored in this study by sEMG examination during the rehabilitation procedure. The usability of these sEMG indicators was confirmed in examining complex neuromuscular changes in patients with stroke during rehabilitation. Moreover, the combination of these indicators was found to provide a more comprehensive insight to underlying mechanisms concerning neuromuscular alternations and their recovery. Through four cases in this pilot study, complex and different neuromuscular processes were illustrated during the monitored rehabilitation procedure, and the order and timing of these neuromuscular processes varied across individuals. Our attempts at

sEMG tracking analysis successfully provides a noninvasive and convenient approach to evaluate the improvement of complex post-stroke neuromuscular changes during rehabilitation process at the individual level, thus offering better guideline for specifical design of more individualized rehabilitation protocol.

Table 1. Demographic information of the stroke subjects.

ID #	Sex	Age (years)	Duration (days)	Paretic side	Dominant side	B stage	F-M	MAS
S1	F	51–55	702	R	R	4	40	0
S2	M	76–80	99	L	R	3	33	0
S3	M	46–50	48	L	R	2	27	0
S4	M	71–75	28	L	R	2	15	0
S5	M	56–60	72	L	R	4	21	0
S6	F	81–85	39	R	R	3	32	0
S7	M	56–60	45	R	R	4	12	0
S8	M	61–65	27	L	R	2	20	0
S9	M	51–55	57	R	R	3	4	0
S10	M	71–75	31	L	R	4	39	0
S11	F	76–80	224	L	R	3	21	0
S12	F	51–55	58	L	R	3	35	0
S13	M	61–65	57	R	R	2	4	0
S14	M	61–65	43	L	R	4	45	0
S15	M	41–45	45	R	R	1	2	0
S16	M	51–55	154	L	R	5	45	0
S17	M	81–85	36	L	R	5	55	0
S18	M	46–50	35	L	R	4	43	1
S19	M	56–50	74	R	R	2	23	0
S20	F	56–60	410	L	R	5	50	0
S21	F	51–55	40	R	R	2	25	0
S22	M	46–50	80	R	R	5	55	0
S23	M	56–60	42	L	R	4	44	0

B stage: Brunnstrom stage; F-M: upper extremity Fugl-Meyer assessment; MAS: modified Ashworth scale

2. Materials and method

2.1. Subjects

Twenty-three subjects with stroke (S1–S23, age: 60 ± 11 years old, ranging from 46–82 years old), 7 age-matched eldly healthy control subjects (C1–C7, age: 60 ± 5 years old, ranging from 55–67 years old) and 11 younger healthy control subjects (C8–C18, age: 24 ± 2 years old, ranging from 22–30 years old) participated in this study. All subjects with stroke were recruited from the inpatient department of rehabilitation medicine in the First Affiliated Hospital of Anhui Medical

University (Hefei, Anhui Province, China). This study was approved by the Ethic Review Committee of the hospital. All stroke patients were diagnosed by Computed Tomography or Magnetic Resonance Imaging scan and confirmed no brain trauma or other neurological diseases (such as multiple sclerosis). For each stroke patient, clinical assessment was performed by the same clinician before the experiment. Both the F-M scale and the modified Ashworth scale (MAS) [42] were used to assess motor function and muscle spasticity of the affected upper-extremities of the subjects with stroke, as shown in Table 1. All the control subjects were healthy volunteers without any known history of neural or muscular disorder. All subjects gave their informed and signed consent before any experimental procedure.

2.2. Experiments protocol

The abductor pollicis brevis (APB) muscle of the thenar eminence was examined by performing thumb abduction (corresponding to the main APB function) in this study. Due to its superficial location, the APB muscle was targeted by two Ag/AgCl disc surface electrodes (10 mm in diameter, JK-1A, JunKang Inc., Shanghai, China) placed over the thenar eminence along muscle fiber at a center-to-center distance of 20mm. A large round reference electrode (Dermatrode; American Imex, Irvine, CA) was placed on the back of the hand on the same side. A self-made sEMG recoding system was built with a two-stage amplifier at a total gain of 60dB and a band-pass filter at 20–500 Hz. This system is the same with the one used in our previous studies with sufficient validation through scientific research [43–45]. The recorded sEMG signals were further digitized in a 24-bit A/D converter (ADS1299, Texas Instruments, TX) with a sample rate of 1 kHz, and displayed on the screen of the computer in a real-time manner to monitor the signal quality and then stored for offline analysis.

The experiments had a protocol to conduct multiple sessions of sEMG examinations for all stroke subjects during their inpatient rehabilitation period, which was expected to be two months. During hospitalization, patients receive appropriate physiotherapy according to their doctor's prescription every morning and afternoon. According to the course of treatment, we chose appropriate time slots to carry out the experiment. Specifically, the execution session of each examination was scheduled two hours before and after the physiotherapeutic treatment, to ensure sufficient rest for the subjects and to avoid temporary changes of MU properties just following the physiotherapy. Moreover, the frequency of repeated examinations was designed to be once per week. In fact, each of the 23 subjects with stroke (S1–S23) participated into at least one session of the examination scheduled at the beginning of the treatment, where muscles on both sides were examined. However, the specific experimental arrangement was restricted by many factors such as time convenience of the subjects. By overcoming difficulties from many parties, 9 of the 23 subjects with stroke (S1–S9) had their paretic muscles examined at least twice, scheduled right at the beginning and the end of the treatment. Finally, 4 of the 9 subjects with stroke (S1–S4) truly completed multiple sessions of sEMG examinations of the paretic muscles during their inpatient rehabilitation treatments. In fact, the number of completed examinations for S1–S4 is 6, 10, 9 and 9, respectively. Each of 18 control subjects (C1–C18) was asked to participate into just a single session of examination, where the subject’s dominant side or non-dominant side was randomly selected.

In order to reduce the interference of environmental noises, experiments were carried out in a quiet testing room. During a single session of the examination, subjects were comfortably seated

with their tested arm bent approximately 90 degrees and placed on a height-adjustable table. The palm of the tested hand should keep flat toward the body, while natural and slight finger flexion was allowed. After securely placing the EMG electrodes, the subjects were then instructed to perform thumb abduction by resisting the force exerted by the experimenter. Maximum voluntary contraction (MVC) of each tested muscle was roughly perceived by the experimenter while the subjects were encouraged to perform muscle contractions with maximal efforts. The determined MVC was used to guide generation of the resistant force at multiple levels. Several data recording trials were conducted in each examination session. In a single trial, the subject was instructed to perform isometric contractions with increasingly graded contraction levels from a very mild level to almost maximal level, roughly corresponding to 10%, 30%, 50%, 70%, submaximal (90%) and almost MVC. For each contraction level, subjects were asked to maintain as stable as possible for at least 3 seconds. Such a trial was repeated for at least 3 times. To avoid muscle fatigue, sufficient rest was allowed between consecutive trials. The recorded raw sEMG data were finally imported into the MATLAB (Version R2015, MathWorks, Natick, USA) software for offline analysis.

2.3. Data analysis

2.3.1. Data preprocessing

The sEMG signals were filtered by a 4th order Butterworth filter with a filter bandwidth of 20–500 Hz to filter motion artifacts, low-frequency baseline drift, and high-frequency noise. Power line interference and its harmonics caused by the power supply in the environment were filtered using a bandwidth adjustable notch filter. In order to obtain the electrophysiological signal during muscle contraction, active segment detection was conducted to the filtered signal. The most critical step in the detection of active segments is to determine the onset and offset of the corresponding signal segment during muscle contraction. This step can be done with an amplitude-based threshold detection method [46], which determines the onset and offset of the signal by comparing the rectified signal amplitude with a selected threshold (typically set to 3 times the standard deviation of the baseline). In a single trial, sEMG signals were divided into non-overlapping epochs at a length of 1s with stable contractions at certain force levels. Finally, approximately 30 epochs for each tested muscle were obtained for further analysis.

2.3.2. Indicators from the sEMG Examination

Three sEMG interference pattern analysis methods were applied for tracking analysis in this study, including CI [47], MDF [32] and RMS [29], as three indicators of neuromuscular status. For each data obtained by a single trial, the results of the three indicators can be given separately. Three indicators were used for double-measurement analysis before and after rehabilitation and multiple measurements during rehabilitation. We will introduce the three indicators, respectively.

2.3.2.1. CI Analysis

CI is used to measure the degree of signal area clustering. CI values range from 0 to 1, and especially high value of CI indicates highly clustered sEMG signal which characterized by isolated

and large MUAPs. As previous studies reported [41], sEMG recorded from muscles with neurogenic changes corresponds to relative high CI values. Moreover, signals with myopathic changes tend to be flat and dense, so the CI value is relatively low [48]. In the CI analysis method proposed by Uesugi [40,47], the sEMG collected under different force level of the subjects are processed into 1s smooth non-overlapping analysis window [48].

In this paper, we intercept 20~40 signal segments with 1s length of contraction force as stable as possible from each activity segment of each subject. In this process, an intensity distribution of epochs from the minimum to the maximum random contraction should be ensured. CI values were calculated for each epoch. The first step in CI calculation is to divide the 1s epoch into non-overlapping windows with the same size [40]. The window length was set at 15 ms, which were recommended to ensure that it covers at least a large and individual MUAP produced by a MU with neurogenic lesion. In this paper, the sampling rate of the signal is 1000Hz, that is, the time series of one window includes 15 sampling points. Finally, K (K = 66) windows are obtained.

The CI is calculated as

$$\mathrm{CI} = \left(\sum_{i=1}^{k-1} DA_i^2 + \sum_{i=1}^{k-2} DB_i^2 + \sum_{i=1}^{k-3} DC_i^2\right)/6 \cdot \sum_{i=1}^{k} A_i^2, \tag{1}$$

where DA_i is the differential sequences between every consecutive area value, DB_i is the differential sequences between every second area value, and DC_i is the differential sequences between every third area value. A_i is the window area.

The normal range employed plots from neither dominant or non-dominant muscles of 18 healthy individuals and contralateral muscles of the 23 stroke patients with single sEMG collection. In fact, it was reported that neuromuscular status of the contralateral muscle from patients with subacute stroke is close to healthy controls, whose plots were almost overlapped over those derived from the control subjects. Moreover, the diagnostic results would be more reliable by enlarging the sample size of the normal range. Therefore, it is feasible to employ plots from contralateral muscles for establishment of normal range. To define the distribution of the normal cloud for judging abnormality, linear regression was performed on double-logarithmic coordinates of normal cloud (see Figure 1, $y = -0.188x - 0.588$). The regression line was a represent to account for the relationship between the CI and muscle force, generally for the normal data. Then, the upright distance between the log(CI) and the regression line was calculated and termed as deviation of the processed epoch. The normal range (dashed lines) is presented within ±2.5 times the standard error of the deviation of all epochs from normal range. On each side of a subject (In this study, the equivalent of each muscle), the data plots of each epoch can obtain a distance to the regression line (residual deviation). Then, the distance values of all the data points of each individual muscle are averaged as the distance from the normal mean value of a single individual data and denoted as mean residual (*Rm*), which then can be used to assess the presence of abnormality for a tested muscle. For further quantification, the mean μ_0 and standard deviation (SD) σ_0 of the *Rm* values for muscles of healthy controls and the contralateral side of all the stroke patients were calculated. Finally, Z-score was calculated for each individual muscle as follows:

$$\mathrm{Z} = \frac{Rm - \mu_0}{\sigma_0} \tag{2}$$

A Z-score within ±2.5 was predefined as normal. Patient with a Z-score higher than +2.5

was diagnosed as being neurogenic changes and a Z-score lower than −2.5 indicated dominant myogenic changes.

2.3.2.2. RMS and MDF Analyses

RMS is a popular time-domain feature for characterizing sEMG signals, representing muscle strength [49]. MDF is a parameter widely used in power spectrum analysis, which reflects main frequency component and spectral structure of a time series signal [34]. Moreover, the MDF calculated from the sEMG signal is a reflection of various neuromuscular changes associated with both central (e.g., altered MU control properties) and peripheral factors (e.g., muscle fiber entropy) [32,34]. The MDF changes of paretic muscles with respect to corresponding contralateral muscles help to reveal neuromuscular alternations. For example, there might be re-innervation of muscle fibers in paretic muscles when their MDF is found to be higher than contralateral muscles [32,34]. On the contrary, paretic muscles with relative lower MDF may suffer from muscle fiber atrophy or decreased MU firing rate [32,34,50].

In this study, both indicators are only calculated on the signals recorded during MVC for each muscle. The MDF is computed from each epoch of simulation and experimental sEMG with the periodogram-based spectrum estimation.

2.4. Statistical analysis

A total of 9 subjects with stroke (S1–S9) successfully completed at least two sessions of the sEMG examinations of the paretic muscles, scheduled at the beginning and end of the treatment procedure. For each of 9 subjects with stroke (S1–S9) completing both the first and final sessions, the absolute differences of the MDF between the paretic muscles and the contralateral muscles were calculated for the first session and the final session, and were denoted as D1 and D2, respectively. A paired t-test was applied between D1 and D2 to evaluate effect of rehabilitation treatment on the MDF values. In addition, in order to investigate whether the RMS, the absolute value of Z-score of CI, and other clinical evaluation scores can reflect the effect of rehabilitation and the recovery of paretic muscles, a series of paired t-tests were was applied to these indicators/scores between the first session and the final session, respectively. Moreover, we calculated the increments between the final session and the first session of the three indicators and the F-M score for paretic muscles of 9 subjects with stroke, denoted them as I_RMS, I_MDF, I_CI and I_FM respectively. In order to evaluate whether and how any of three indicators was correlated with the clinical assessment scale, a series of correlation analyses were performed between the I_FM and each of the three indicator increments (I_RMS, I_MDF and I_CI). In addition, independent sample t-tests was performed of the Z-scores of CI indicator between 11 young healthy subjects and 7 age-matched elderly healthy subjects to examine the effect of age on the CI values. The significant level was set to be $p < 0.05$. All the tests were completed using SPSS software (ver. 16.0, SPSS Inc. Chicago, IL, USA).

3. Results

Figure 1 illustrates the CI-area plots from three different muscles. The normal range was established with data from any muscles of the 18 healthy individuals and the contralateral muscles of

the 23 subjects with stroke in a single examination session at the beginning of the treatments. Most data points from the paretic muscles of the subjects with stroke were distributed in the normal range, whereas a small number of data points were distributed outside in particular. In addition, independent sample t-tests reported that no significant difference in both variance (p = 0.524) and mean (p = 0.122) of the Z-scores of CI between the 11 young healthy subjects and 7 elderly healthy subjects. This confirmed the correctness of establishing the CI normal limits by pooling all the data of both eldly and younger control subjects.

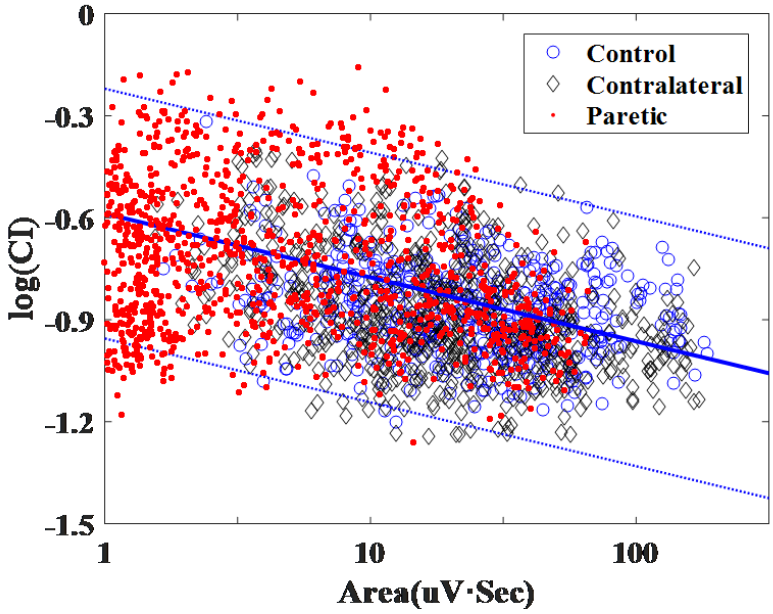

Figure 1. The CI-area plot presented in double logarithmic scale, and the CI-area plot from both the (blue circle) 18 healthy control subjects and the contralateral side (black diamond) and the paretic side (red dot) of all 23 subjects with stroke. The regression analysis (blue solid line) was performed on normal data consisting of epochs (1≤total area≤100uVsec) from normal range. The normal range (dashed lines) is presented within ±2.5 times the standard error of the linear regression.

Figure 2 shows values of three sEMG indicators and the F-M score obtained at the first session and the final session for 9 subjects with stroke, respectively. Paired T-tests analysis reported a significant main difference between both sessions for the F-M score (T = −6.275, p = 0.000) and the MDF (T = 3.502, p = 0.008) derived from the paretic muscles. However, the sEMG RMS (T = −1.901, p = 0.094) and Z-score of CI (T = 1.618, p = 0.144) did not report any significance. In details, the mean value of MDF (from 26.4222 to 10.3344) and mean Z-score of CI (from 1.8011 to 0.9855) were reduced and meanwhile the mean value of RMS (from 31.6211 to 55.6989) was increased after the rehabilitation therapy. In addition, correlation analyses reported that no significant correlation was observed between the increment of the F-M score and the increment of the RMS (r = 0.293, p = 0.445), the increment of MDF (r = 0.174, p= 0.655) and the increment of Z-score of CI (r= 0.196, p = 0.613), respectively.

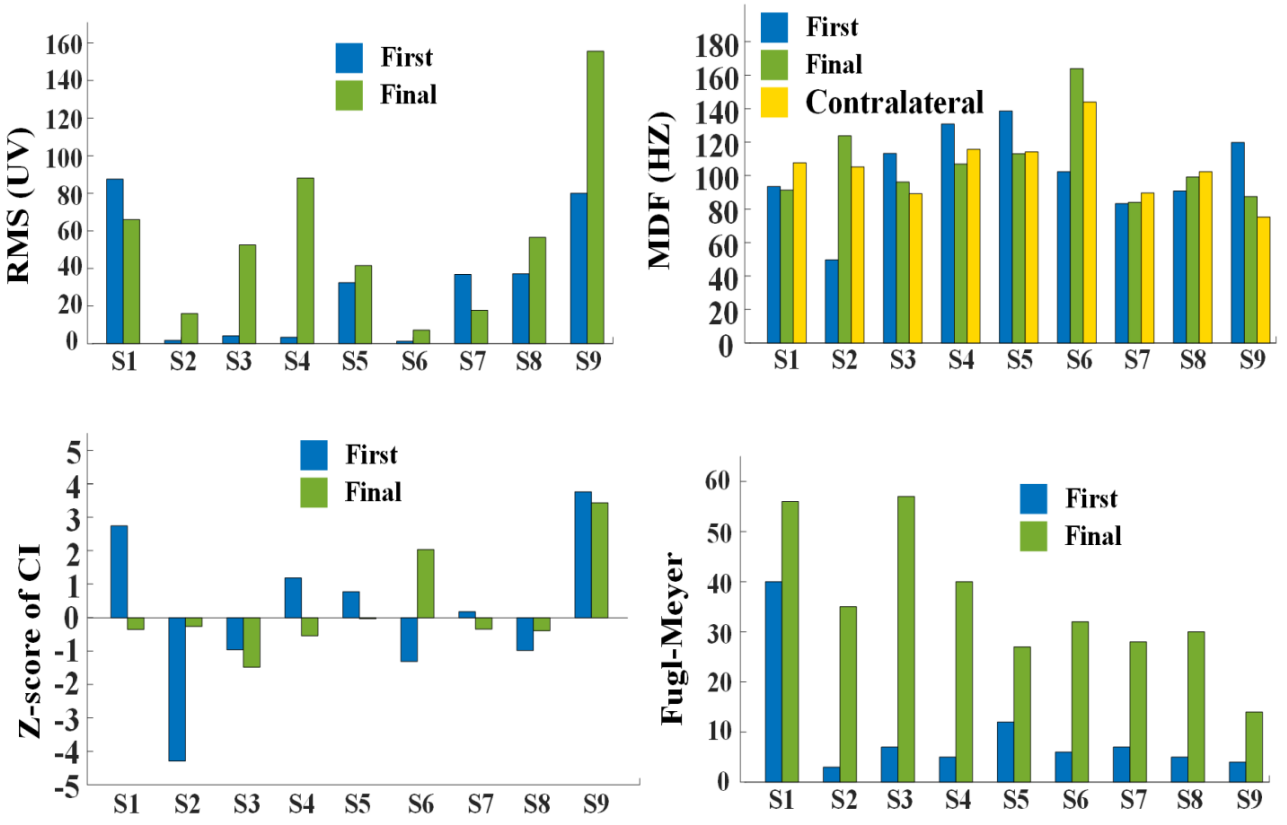

Figure 2. Results of three sEMG indicators and the Fugl-Meyer assessment scores for 9 subjects with stroke (S1-S9), at the first and the final examination sessions, respectively. For the sEMG MDF, the MDF values from the contralateral muscles are reported as well.

Figure 3 reports the curves of three sEMG indicators derived from the monitoring of paretic muscles during the rehabilitation procedure for four subjects with stroke. For the subject S1, both the RMS curve and the MDF curve values derived from the subject's paretic muscle had an almost flat trend with slight variations. However, the Z-scores of CI for S1 kept falling down from neurogenic abnormality to the normal range. For the subject S2, the first examination at the beginning of the treatment reported low MDF and abnormally low Z-score of CI for the paretic muscle of the subject. Subsequently, the MDF exhibited an increasing trend during the first stage, and meanwhile Z-scores of CI increased significantly from the lower abnormality area through the normal range even to upper abnormality area. During the later stage, with further rehabilitation treatment, both RMS and MDF curves had slight fluctuations and a generally slight increasing trend, and Z-scores of CI fell down within the normal range. For the subject S3, the RMS curve derived from the paretic muscle of the subject S4 obviously climbed up to the level of corresponding contralateral muscle. By contrast, other two indicators did not change a lot. For the subject S4, in the first 25 days since stroke onset, MDF of the paretic muscle dropped sharply towards that of the contralateral muscle, and observed that the RMS curve was on the rise. Meanwhile, the Z-score of CI fluctuated slightly within the normal range during the treatment. During the later stage after 25 days post stroke, the RMS curve kept climbing up whereas the other two curves of the paretic muscles remains almost unchanged.

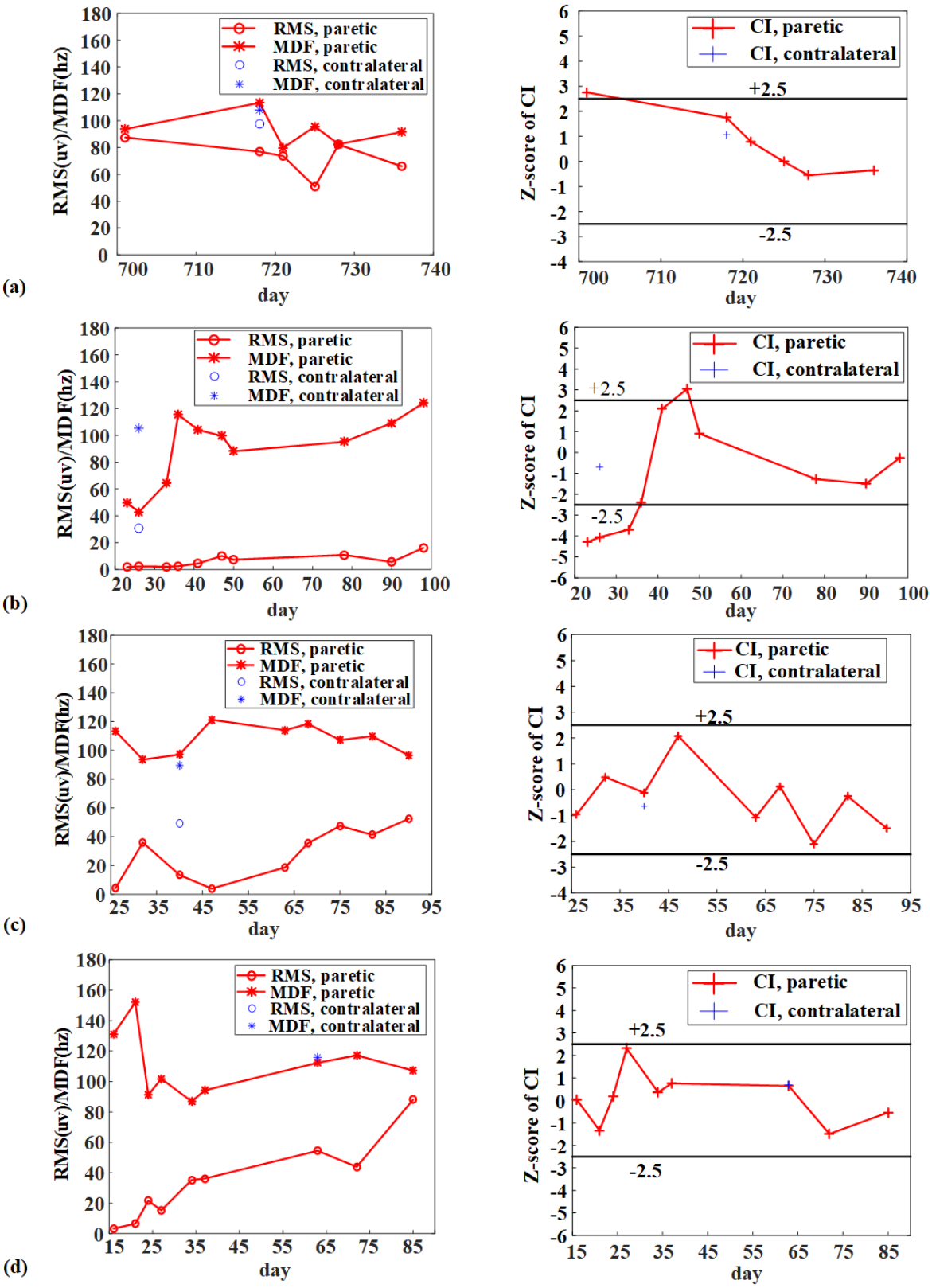

Figure 3. Three sEMG indicator curves derived from monitoring paretic muscles of S1(a), S2(b), S3(c), S4(d) during the rehabilitation treatment. Those indicator values from the corresponding contralateral muscles are shown with isolated symbols as the reference.

4. Discussion

In this paper, three indicators derived from sEMG examination were used to monitor complex neuromuscular changes in paretic muscles of subjects with stroke during rehabilitation treatments. As a pilot study, only 4 cases preliminarily completed the monitoring and tracking analysis protocol and they are reported in this paper. Prior to the tracking analyses, the data from 18 healthy control subjects and the data from a single test on the contralateral side of 23 stroke patients, were pooled together to form the diagnostic criteria of CI method, which is the basis of using this method in tracking data analysis. When a single test was just performed, the Z-scores of CI obtained from paretic muscles of all subjects with stroke showed a very board distribution pattern from abnormally low values through normality to abnormally high values. This finding was consistent with our previous work [41], confirming the diversity of neuromuscular changes after stroke. A variety of neuromuscular changes have been reported in the literature, contributing to sEMG abnormalities following stroke. Review of these changes, both central and peripheral, helps to establish examination criteria given combination of three indicators. Specifically, RMS used in this study can be regarded to reflect capability of producing muscle strength. Decreased strength of paretic muscles is primarily associated with a deficit of descending central drive as a result of central nervous impairment [51], while various other changes may also contribute. The general changing trends of the MDF and CI with neuromuscular changes are shown in Table 2. The relative increase of MDF in paretic muscles as compared to corresponding contralateral muscles may be related to reorganization of the MU architecture (e.g. re-innervation of muscle fibers) [8,9,32,34], resulting in enlargement of a proportion of the remaining MUs [20,34,52,53]. By contrast, the relative decrease of MDF may be attributed into decreased number of MUs that are capable of being activated [32,53,54], selective loss or deactivation of larger and superficial MUs [34], changes in central control properties (including MU firing rate reduction [32,34,55,56], firing synchronization increase [32,57,58]) and atrophy of muscle fibers [34,50]. Please note that the decreased number of activable MUs can be contributed by two factors, given examination of voluntary EMG. One is the loss of MUs, which is due to the trans-synaptic degeneration of α-motor neurons [41,53,54]. In the other factor, some MUs fail to be activated to function properly, although they are anatomically intact, which is due to modification of MUs' relationship within the motor neuron pool, not permanent degeneration of lower/spinal motor neurons. Therefore, this phenomenon was termed as decreased number of activiable MUs rather than loss of MUs. The CI method has been reported to have a different examination criteria. Abnormal increase of CI (i.e., Z-score of CI) may be associated with decreased number of activable MUs [41,53,54], changes in central control properties (including MU firing rate reduction [41,55,56], firing synchronization increase [41,57,58] and recruitment range compression [31,41,59]) and muscle fiber re-innervation [8,9,41] to produce enlarged MUs, all of which are factors indicating neurogenic changes. Meanwhile, abnormal decrease of CI may be represents that atrophy of muscle fibers, especially type II fiber atrophy [8,41] (which is myopathic), and selected loss of larger MUs [41,60] is likely to take place in paretic muscles following stroke. All the indicators and their criteria were used as examination tools in this pilot study. On this basis, any possible abnormalities can be better interpreted with a special tracking and monitoring experimental protocol.

Among the 23 subjects with stroke, 9 of them have their paretic muscles tested at least twice, i.e., before and after the rehabilitation treatment. In pre- and post-treatment comparison, the changing

trend of three indicators as well as the clinical F-M scale truly reflects positive effect of the rehabilitation treatment with improvement in paretic muscle functions. In detail, the RMS values of the paretic muscles were found to generally rise up. Regardless of increase or decrease of the MDF values in the paretic muscles, they tended to approach to those values in the corresponding contralateral/unimpaired muscles. Similarly, paretic muscles had their Z-scores of CI return to the normal range, a small range beside 0, from abnormality beyond +2.5 or below −2.5. All these findings give a general verification of our hypothesis regarding the usability of the sEMG analyses with three indicators in examining therapeutic effect during rehabilitation procedure.

Table 2. General changing trend of both sEMG indicators.

Neuromuscular Changes	MDF	CI
Decreased number of MUs	decrease [32, 53, 54]	increase [41, 53, 54]
Selective loss or deactivation of larger and superficial MUs	decrease [34]	decrease [41, 60]
MU firing rate reduction	decrease [32, 34, 55, 56]	increase [41, 55, 56]
Firing synchronization	decrease [32, 57, 58]	increase [41, 57, 58]
Recruitment range compression	probably insensitive	increase [31, 41, 59]
Atrophy of muscle fibers	decrease [34, 50]	decrease [8, 41, 60]
Re-innervation of muscle fibers	increase [8, 9, 32, 34]	increase [8, 9, 41]

Moreover, the increment of any sEMG indicator was found to be not significantly correlated with the increment of F-M score during the entire rehabilitation procedure ($p>0.05$). It should be acknowledged that both sEMG examination and clinical F-M scale evaluate different aspects of muscle functions. The sEMG analysis is used to examine detailed neuromuscular changes, whereas the clinical F-M scale mainly quantifies gross motor functions of the paretic muscles. This can be used to explain no correlation between them even for a group of the same subjects.

Following the protocol for monitoring paretic muscle changes, 4 of 23 subjects with stroke successfully participated into repeated examinations of their paretic muscles during the rehabilitation treatment. Each of four subjects showed a distinct recovery procedure regarding the curves of all sEMG indicators. Among these four subjects, the subject S1 showed a relatively simple trend with slight variations of both RMS and MDF curves of the examined paretic muscles. However, the Z-scores of CI for S1 kept falling down from neurogenic abnormality to the normal range. Combination of changing trends of all three sEMG indicators is likely to indicate all possible neurogenic changes (e.g. altered central control properties) that previously took place might be gradually recovered. It is worth noting that the weak variation of the subject S1's RMS and MDF values during rehabilitation treatment might be related to the long-term duration since stroke onset. The physical characteristics of the subject in this chronic stage remained to be stable with slow improvement of motor functions. This was confirmed by the F-M score, which was obviously high before the treatment with a limited increase after the treatment for the subject S1. Insensitivity of both RMS and MDF to these sligh improvements also explains almost flat trend of both indicators.

For the subject S2, the resultant three-indicator curves were much more informative, as compared with results of two tests just before and after the treatment. By visual inspection, the rehabilitation procedure of the subject S2 can be divided into two stages. The first stage began from

the treatment (on the 23rd day) to the 46th day since stroke onset. The first examination at the beginning of the treatment reported low MDF and abnormally low Z-score of CI for the paretic muscle of the subject, indicating that selective loss or deactivation of larger MUs [34,41,60] and therefore possible muscle fiber denervation and fiber type grouping [7,8,32,41,61] were very likely to occur in the paretic muscle. Subsequently, the MDF exhibited an increasing trend during the first stage, and meanwhile Z-scores of CI increased significantly from the lower abnormality area through the normal range even to upper abnormality area. Reasons for explaining these phenomena possibly include recalling of larger MUs as a result of central neural plasticity [8,41,60], and both re-innervation of previously denervated muscle fibers and remodeling of MUs [8,9,32,41] considered as peripheral compensation for previous decreased number of larger MUs [34,41,60]. These phenomena really help to contribute into paretic muscle recovery in the first stage. In this stage, alternations in control properties might take place or even be developed concurrently as a result of lesions to central nervous system, especially leading to abnormaly high CI around the 46thy day. The second stage continued till the end of treatment on the 98th day since stroke onset. With further rehabilitation treatment, both RMS and MDF curves had a generally increasing trend, and meanwhile Z-scores of CI fell down within the normal range. It can be speculated that previously damaged central control properties [32,34,41,55–58] might be gradually recovered during this stage. Ongoing central neural plasticity may also lead to recovery of descending central drives and increased number of MU to be activated [32,41,53,54], which generally contribute to recovery of paretic muscle functions for the subject S2.

The RMS curve derived from the paretic muscle of the subject S3 obviously climbed up to the level of corresponding contralateral muscle. By contrast, other two indicators did not change a lot, remains around the value of contralateral muscle (for MDF) and within the normal range (for Z-score of CI). The probable cause is the more or less normal function of the paretic muscle. In this condition, initially impaired muscle strength was likely due to a deficit of descending central drive, and its recovery as a result of central plasticity contributed into the significant therapeutic effect [51].

The motor recovery of S4 obviously had a stage-dependent character as well due to high variations in order and timing of fluctuations of the three-indicator curves. In the first 25 days since stroke onset, MDF of the paretic muscle dropped sharply towards that of the contralateral muscle, and an increasing trend of the RMS curve was observed. Meanwhile, the Z-score of CI fluctuated slightly within the normal range during the treatment. The probable process underlying the first-stage treatment is the gradual recovery of the decreased number of activated MUs [32,41,53,54]. It can be speculated that severe decreased number of activable MUs might be a possible factor contributing into the initial muscle impairment. As a compensation, muscle contraction had to recruit a more portion of larger/enlarged MUs with higher muscle fiber conduction velocity [34,62] and sharper MUAP waveforms [34,59], thus resulting in abnormally increased MDF values before the treatment. In a later stage after 25 days post stroke, the RMS curve kept climbing up whereas the other two curves of the paretic muscles remains almost unchanged with further application of the rehabilitation protocol. These three-indicator curves show a similar pattern to that of the subject S3, thus with the same reasons for explaining the therapeutic effect, as discussed in above paragraph.

Beside the confirmed usability of three indicators, their different sensitivities to various types of neuromuscular changes are further reported and explained. It is demonstrated that the combination of three indicators truly helped to enhance the examination power in discriminating specific neuromuscular changes, given their complementary capabilities of revealing complex paretic muscle

changes. Our pilot study highlights the combined use of three indicators in monitoring the individual rehabilitation treatments in terms of recovery of paretic muscle changes, which was demonstrated by monitoring the outcomes in four cases as typical examples.

Moreover, through the 4 subjects with stroke successfully participated into repeated examinations of their paretic muscles, we preliminarily found that there is a great diversity of neuromuscular changes, and different individuals have different changes during rehabilitation treatment. Seen from S1 and S2, the leading pathogen is different among individuals, so the process of neuromuscular change is different. We also found that the order and timing of neuromuscular processes contributing to recovery of paretic muscles were quite different from each other, so the sEMG examination tools proposed in this paper is more meaningful for personalized treatment during rehabilitation treatment. Above findings may be related to different severity in brain lesion after stroke. In a word, this exactly indicates that it is essential to track and monitor the paretic muscles of individuals, thus offering important guideline for promoting motor recovery.

However, some limitations still exist in this paper. Our work focuses on the development of sEMG indicators for monitoring complex neuromuscular changes in paretic muscles of patients with stroke. It should be noted that at the expenses of quick and noninvasive implementation, the sEMG analyses have limitations in quantifying specific MU properties. Although the three adopted indicators give a useful assessment of complex neuromuscular changes in paretic muscles, more analytical methods such as EMG decomposition at MU level and muscle biopsy are required to offer more information. In addition, unsupervised learning has been widely used in the field of biomedicine (e.g. genetic detecting [63], gene expression data [64, 65] and disease diagnosis [66]). Therefore, we can also try to use unsupervised learning to assess complex neuromuscular changes in patients with stroke during rehabilitation in the future. Moreover, there may be inconsistencies in the assessment results of three indicators used in this pilot study. They can be attributed into some unrevealed neuromuscular changes or concurrent appearance of complex processes. As previously hypothesized in this study, the neuromuscular processes become even more complicated by considering a long time course of rehabilitation treatment. Therefore, it is necessary to combine more effective indiators toward precise interpretations of the examination results. It is also required to enrich the small sample size (i.e., 4) of the subjects who successfully completed the tracking protocol with multiple sessions. In general, this study only preliminarily demonstrates the feasibility of monitoring complex neuromuscular processes using sEMG examination in paretic muscles of patients with stroke during their rehabilitation. Our future efforts will focus on these above-mentioned directions to enchance usability of the sEMG examination tools and to enrich our knowledge regarding underneath mechanisms of stroke rehabilitation beyond the currently preliminary findings.

5. Conclusion

In summary, this pilot study reports four cases to illustrate complex and different neuromuscular processes during their rehabilitation procedure monitored by three sEMG indicators. Specifically, these progressive processes were found to vary in timing and order across individuals, mainly associated with the original types of stroke-induced neuromuscular changes at the MU level, including decreased number of activable MUs, alternations in the structure of MUs and the altered central control properties of MUs. The proposed multi-parameter sEMG tracking analysis provides a

convenient and effective approach to understand the complex neuromuscular changes in patients with stroke, and helps to view the improvement of MU alternations during the rehabilitation process, thus offering guidelines for a better design of individualized stroke rehabilitation protocol.

Acknowledgments

We appreciate the subjects with stroke and healthy control subjects for participating in this research. We also thank the doctors, therapists, and nurses for their assistance in the experiment. Finally, we would like to thank our team members and tutors for their help in data collection and article modification. This work was supported by the National Nature Science Foundation of China (Grant number: 61771444).

Conflict of interest

The authors declare that the research was conducted in the absence of any commercial or financial relationships that could be construed as a potential conflict of interest.

References

1. S. Mendis, Stroke disability and rehabilitation of stroke: World Health Organization perspective, *Int. J. Stroke*, **8** (2013), 3–4.
2. D. T. Wade, Measurement in neurological rehabilitation, *Curr. Opin. Neurol.*, **5** (1992), 682–686.
3. P. Langhorne, F. Coupar and A. Pollock, Motor recovery after stroke: A systematic review, *Lancet Neurol.*, **8** (2009), 741–754.
4. G. Kwakkel, B. Kollen and E. Linderman, Understanding the pattern of functional recovery after stroke: facts and theories, *Restor. Neurol. Neurosci.*, **22** (2004), 281–299.
5. R. H. Nijland, E. Wegen, H. Wel, et al., Presence of finger extension and shoulder abduction within 72 hours after stroke predicts functional recovery. Early prediction of functional outcome after stroke: the EPOS cohort study, *Stroke*, **41** (2010), 745–750.
6. R. H. Nijland, E. Wegen, J. Verbunt, et al., A comparison of two validated tests for upper limb function after stroke: the Wolf Motor Function Test and the Action Research Arm Test, *J. Rehabil. Med.*, **42** (2010), 694–696.
7. L. Brewer, F. Horgan, A. Hickey, et al., Stroke rehabilitation: Recent advances and future therapies, *QJM*, **106**, (2013), 11–25.
8. R. Dattola, P. Girlanda, G. Vita, et al., Muscle rearrangement in patients with hemiparesis after stroke: an electrophysiological and morphological study, *Eur. Neurol.*, **33** (1993), 109–114.
9. R. P. Segura and V. Sahgal, Hemiplegic atrophy: Electrophysiological and morphological studies, *Muscle Nerve*, **4** (1981), 246–248.
10. C. W. Chang, Evident trans-synaptic degeneration of motor neurons after stroke: A study of neuromuscular jitter by axonal microstimulation, *Electroencephalogr. Clin. Neurophysiol*, **109** (1998), 199–202.
11. M. Lukács, L. Vécsei and S. Beniczky, Changes in muscle fiber density following a stroke, *Clin. Neurophysiol.*, **120** (2009), 1539–1542.
12. C. Bérard, C. Payan, J. Fermanian, et al., A motor function measure scale for neuromuscular diseases. Construction and validation study, *Neuromuscular Disorders*, **15** (2005), 463–470.

13. S. Brunnstrom and D. Carson, Movement therapy in hemiplegia: A neurophysiological approach, *Gerontologist*, **12** (1970).
14. A. R. Fugl-Meyer, L. Jaasko, I. Leyman, et al., The poststroke hemiplegic patient. 1. A method for evaluation of physical performance, *Scand. J. Rehabil. Med.*, **7** (1975), 13–31.
15. F. I. Mahoney, Functional evaluation (the Barthel Index), *Md. State Med. J.*, **14** (1965), 61-65.
16. T. Brott, H. P. Adams, C. P. Olinger, et al., Measurements of acute cerebral infarction: A clinical examination scale, *Stroke*, **20** (1989), 864–870.
17. T. Brott, J. R. Marler, C. P. Olinger, et al., Measurements of acute cerebral infarction: Lesion size by computed tomography, *Stroke*, **20** (1989), 871–875.
18. P. Lyden, T. Brott, B. Tilley, et al., Improved reliability of the NIH Stroke Scale using video training. NINDS TPA Stroke Study Group, *Stroke*, **25** (1994), 2220–2226.
19. A. Fugl-Meyer, L. Jaasko, S. Olsson, et al., The post-stroke hemiplegic patient—Part1: A method for evaluation of physical performance, *Scand. J. Rehabil. Med.*, **7** (1975), 13–31.
20. D. Gladstone, C. Danells and S. Black, The Fugl–Meyer assessment of motor recovery after stroke: A critical review of its measurement properties, *Neurorehabil. Neural Repair*, **16** (2002), 232–240.
21. T. Adel and D. Stashuk, Clinical Quantitative Electromyography, in *Electrodiagnosis in New Frontiers of Clinical Research*, IntechOpen, (2013).
22. M. Lukács, Electrophysiological signs of changes in motor units after ischaemic stroke, *Clin. Neurophysiol.*, **116** (2005), 1566–1570.
23. T. Artuğ, O. Osman, İ. Göker, et al., Classification of neuromuscular diseases in neuromuscular junction and tendon recordings with needle EMG by using Welch's method, *Med. Technol. Nat. Congress IEEE*, (2017), 1–4.
24. C. S. Bickel, C. M. Gregory and J. C. Dean, Motor unit recruitment during neuromuscular electrical stimulation: a critical appraisal, *Eur. J. Appl. Physiol.*, **111** (2011), 2399.
25. C. A. Knight and G. Kamen, Superficial motor units are larger than deeper motor units in human vastus lateralis muscle, *Muscle Nerve*, **31** (2005), 475–480.
26. P. Sbriccoli, F. Felici, A. Rosponi, et al., Exercise induced muscle damage and recovery assessed by means of linear and non-linear sEMG analysis and ultrasonography, *J. Electromyogr. Kinesiol.*, **11** (2001), 73–83.
27. A. Holtermann, C. Grönlund, J. S. Karlsson, et al., Motor unit synchronization during fatigue: described with a novel sEMG method based on large motor unit samples, *J. Electromyogr. Kinesiol.*, **19** (2009), 232–241.
28. F. Palermo, M. Cognolato, A. Gijsberts, et al., Repeatability of grasp recognition for robotic hand prosthesis control based on sEMG data, *IEEE Int. Conf. Rehabil. Robot*, (2017), 1154.
29. J. Y. Hogrel, Clinical applications of surface electromyography in neuromuscular disorders, *Neurophysiol. Clin.*, **35** (2005), 59–71.
30. C. J. Luca, Physiology and mathematics of myoelectric signals, *IEEE Trans. Biomed. Eng.*, **26** (1979), 313–325.
31. X. Li, A. Suresh, P. Zhou, et al., Alterations in the peak amplitude distribution of the surface electromyogram poststroke, *IEEE Trans. Biomed. Eng.*, **60** (2013), 845–852.
32. B. Yao, X. Zhang, S. Li, et al., Analysis of linear electrode array EMG for assessment of hemiparetic biceps brachii muscles, *Front. Hum. Neurosci.*, **9** (2015), 569.
33. S. Karlsson and B. Gerdle, Mean frequency and signal amplitude of the surface EMG of the quadriceps muscles increase with increasing torque—a study using the continuous wavelet

transform, *J. Electromyogr. Kinesiol.*, **11** (2001), 131–140.
34. X. Li, H. Shin, P. Zhou, et al., Power spectral analysis of surface electromyography (EMG) at matched contraction levels of the first dorsal interosseous muscle in stroke survivors, *Clin. Neurophysiol.*, **125** (2014), 988–994.
35. N. S. Arikidis, E. W. Abel and A. Forster, Interscale wavelet maximum-a fine to coarse algorithm for wavelet analysis of the EMG interference pattern, *IEEE Trans. Biomed. Eng.*, **49** (2002), 337–344.
36. A. I. Meigal, S. Rissanen, M. P. Tarvainen, et al., Novel parameters of surface EMG in patients with Parkinson's disease and healthy young and old controls, *J. Electromyogr. Kinesiol.*, **19** (2009), 206–213.
37. W. Chen, Z. Wang, H. Xie, et al., Characterization of surface EMG signal based on fuzzy entropy, *IEEE Trans. Neural Syst. Rehabil. Eng.*, **15** (2007), 266–272.
38. P. A. Kaplanis, C. S. Pattichis and D. Zazula, Multiscale entropy-based approach to automated surface EMG classification of neuromuscular disorders, *Med. Biol. Eng. Comput.*, **48** (2010), 773–781.
39. X. Zhang, P. E. Barkhaus, W. Z. Rymer, et al., Machine learning for supporting diagnosis of amyotrophic lateral sclerosis using surface electromyogram, *IEEE Trans. Neural Syst. Rehabil. Eng.*, **22** (2014), 96–103.
40. M. Higashihara, M. Sonoo, T. Yamamoto, et al., Evaluation of spinal and bulbar muscular atrophy by the clustering index method, *Muscle Nerve*, **44** (2011), 539–546.
41. X. Zhang, Z. Wei, X. Ren, et al., Complex Neuromuscular changes post-stroke revealed by clustering index analysis of surface electromyogram, *IEEE Trans. Neural Syst. Rehabil. Eng.*, **25** (2017), 2105–2112.
42. J. M. Gregson, M. Leathley, A. P. Moore, et al., Reliability of the tone assessment scale and the modified ashworth scale as clinical tools for assessing poststroke spasticity, *Arch. Phys. Med. Rehabil.*, **80** (1999), 1013–1016.
43. C. Huang, X. Chen, S. Cao, et al., An isometric muscle force estimation framework based on a high-density surface EMG array and an NMF algorithm, *J. Neural Eng.*, **14** (2017), 046005.
44. W. Tang, X. Zhang, X. Tang, et al., surface electromyographic examination of Poststroke neuromuscular changes in Proximal and Distal Muscles Using clustering index analysis, *Front. Neurol.*, **8** (2018), 731.
45. X. Tang, X. Zhang, X. Gao, et al., A novel interpretation of sample entropy in surface electromyographic examination of complex neuromuscular alternations in subacute and chronic stroke, *IEEE Trans. Neural Syst. Rehabil. Eng.*, **26** (2018), 1878–1888.
46. P. W. Hodges and B. H. Bui, A comparison of computer-based methods for the determination of onset of muscle contraction using electromyography, *Electroencephalogr. Clin. Neurophysiol.*, **101** (1996), 511–519.
47. H. Uesugi, M. Sonoo, E. Stålberg, et al., "Clustering Index method": A new technique for differentiation between neurogenic and myopathic changes using surface EMG, *Clin. Neurophysiol.*, **122** (2011), 1032–1041.
48. X. Zhang and P. Zhou, Clustering index analysis of the surface electromyogram poststroke, *International IEEE/EMBS Conference on Neural Engineering*, (2013), 1586–1589.
49. J. H. Lawrence and C. J. Luca, Myoelectric signal versus force relationship in different human muscles, *J. Appl. Physiol. Respir. Environ. Exerc. Physiol.*, **54** (1983), 1653–1659.

50. X. L. Hu, K. Y. Tong and L. K. Hung, Firing properties of motor units during fatigue in subjects after stroke, *J. Electromyogr. Kinesiol.*, **16** (2006), 469–476.
51. M. S. Fimland, P. M. Moen, T. Hill et al., Neuromuscular performance of paretic versus non-paretic plantar flexors after stroke, *Eur. J. Appl. Physiol.*, **111** (2011), 3041–3049.
52. A. C. Martinez, F. Campo, M. R. Mingo, et al., Altered motor unit architecture in hemiparetic patients. A single fibre EMG study, *J. Neurol. Neurosurg. Psychiatry*, **45** (1982), 756.
53. S. Chokroverty, M. G. Reyes, F. A. Rubino, et al., Hemiplegic amyotrophy: Muscle and motor point biopsy study, *Arch. Neurol.*, **33** (1976), 104–110.
54. Y. Hara, Y. Masakado and N. Chino, The physiological functional loss of single thenar motor units in the stroke patients: when does it occur? Does it progress?, *Clin. Neurophysiol.*, **115** (2004), 97–103.
55. J. J. Gemperline, S. Allen, D. Walk, et al., Characteristics of motor unit discharge in subjects with hemiparesis, *Muscle Nerve*, **18** (1995), 1101–1114.
56. X. Li, A. Holobar, M. Gazzoni, et al., Examination of poststroke alteration in motor unit firing behavior using high-density surface EMG decomposition, *IEEE Trans. Biomed. Eng*, **62** (2015), 1242–1252.
57. A. K. Datta, S. F. Farmer and J. A. Stephens, Central nervous pathways underlying synchronization of human motor unit firing studied during voluntary contractions, *J. Physiol.*, **432** (1991), 401–425.
58. I. Hausmanowa-Petrusewicz and J. Kopec, EMG parameters changes in the effort pattern at various loads in diseased muscle, *Electromyogr. Clin. Neurophysiol.*, **23** (1983), 213–228.
59. P. Zhou, N. L. Suresh and W. Z. Rymer, Model based sensitivity analysis of EMG–force relation with respect to motor unit properties: applications to muscle paresis in stroke, *Ann. Biomed. Eng.*, **35** (2007), 1521–1531.
60. M. Lukacs, L. Vécsei and S. Beniczky, Large motor units are selectively affected following a stroke, *Clin. Neurophysiol.*, **119** (2008), 2555–2558.
61. E. Stalberg, Electrogenesis in human dystrophic muscle, In: L. P. Rowland, *Pathogenesis of human* muscular *dystrophies*, (1977), 570–587.
62. R. Dengler, R. B. Stein and C. K. Thomas, Axonal conduction velocity and force of single human motor units, *Muscle Nerve*, **11** (1988), 136–145.
63. J. Xi, A. Li and M, Wang, A novel unsupervised learning model for detecting driver genes from pan-cancer data through matrix tri-factorization framework with pairwise similarities constraints, *Neurocomputing*, **296** (2018), 64–73.
64. Q. Huang, X. Huang, Z. Kong, et al., Bi-Phase evolutionary searching for biclusters in gene expression data, *IEEE Trans. Evol. Comput.*, **In press**, (2018).
65. Q. Huang, D. Tao, X. Li, et al., Parallelized evolutionary learning for detection of biclusters in *gene expression data, IEEE/ACM Trans. Comput. Biol. Bioinform.*, **9** (2012), 560–570.
66. G. Singh and L. Samavedham, Unsupervised learning based feature extraction for differential diagnosis of neurodegenerative diseases: A case study on early-stage diagnosis of Parkinson disease, *J. Neurosci. Methods*, **256** (2015), 30–40.

AIMS Press